Article

Low-Frequency Corrosion Fatigue Test Study of Sucker Rods under High-Salinity Well Fluids in Deep CBM Wells

Fenna Zhang [1], Chuankai Jing [1,*], Jia Li [1], Bin Wang [1], Mingwei Ma [1], Tiantian Yi [1] and Hao Hu [2]

[1] College of Mechanical and Electronic Engineering, China University of Petroleum (East China), Qingdao 266580, China; zhangfenna@163.com (F.Z.); li13675482@163.com (J.L.); wangbin152699@163.com (B.W.); mmw0922@163.com (M.M.); yi18940311319@163.com (T.Y.)

[2] China United Coalbed Methane Corp., Ltd., Taiyuan 030032, China; huhao10@cnooc.com.cn

* Correspondence: jingchuank@163.com

Abstract: Corrosion fatigue test is the most direct and effective method to study the corrosion fatigue characteristics of sucker rod. At present, the commonly used test method is the high frequency fatigue test, but the working state of sucker rod is typical low-frequency and high-cycle corrosion fatigue, and the test with high frequency will reduce the impact of corrosion. Alloy steel 4330 is widely used in coalbed gas well high strength sucker rod, but the research on its low frequency corrosion fatigue life is relatively few. Therefore, in this paper, the corrosion fatigue test method of axial low-frequency and high-cycle was adopted to study the corrosion fatigue characteristics of 4330 steel sucker rod through the corrosion fatigue test under different typical corrosion media, temperature, and stress levels. The results show that the fatigue life of 4330 sucker rod drops sharply when the Cl^- concentration in high salinity well fluid exceeds the threshold value of 155 mg/L. When this threshold is exceeded, the downward trend slows down. It can be seen that the significant factor affecting the corrosion fatigue life of 4330 material is not the concentration of Cl^-, but the existence of Cl^-. The presence of HCO_3^- promotes a further decrease in the corrosion fatigue life of the 4330 sucker rod by Cl^-. The corrosion fatigue life of 4330 sucker rod decreases with the increase of temperature. When the well fluid temperature is less than 50 °C, the impact is relatively significant. When the well fluid temperature is more than 70 °C, the decline trend of corrosion fatigue life slows down. Based on the fitted S-N curve (stress-fatigue life curve), it is calculated that the fatigue limit of 4330 sucker rod at the stress ratio of 0.6 is 196 MPa in the solution of 10,000 mg/L Cl^- at room temperature. These could provide valuable theoretical and technical guidance for design and selection of high-strength sucker rod in high-salinity corrosion well fluid environment.

Keywords: deep CBM wells; high-salinity; low-frequency corrosion fatigue; S-N curve; 4330 sucker rod

1. Introduction

CBM (coal bed methane) is one of the most important unconventional oil and gas resources. The development of coalbed methane can not only provide clean energy for the country and alleviate the shortage of clean energy, but also reduce coal mine gas accidents and greenhouse gas emissions [1]. Coal reservoir permeability is one of the key parameters affecting the recoverability of coalbed methane. Bao Jia proposed that nanopore confinement leads to low matched permeability due to reduced viscosity in the matrix-only porous media. The fracture-matrix system complicates the interpretation of nanopore constraint impact on flow behavior in shale reservoirs [2]. The drainage and production system composed of a pumping rod, pumping pump, and a pumping unit is an important drainage and production mode of coal bed methane wells, accounting for more than 80% of the drainage and production mode of coal bed methane wells. The pumping rod is used to transfer the energy output by the pumping unit to the underground pumping pump to lift the coal seam-produced water to the ground [3–5]. With the development of

coal bed methane wells towards deep coal seams, such as the Daji deep coal bed methane field in China, the average stress and stress amplitude of the pumping rod string are greatly increased due to the continuous deepening of pumping and large liquid production. Therefore, the high strength pumping rod has been preliminarily used. Under the action of alternating stress when the sucker rod is working combined with the high salinity of the produced water from the deep coal bed methane well, the well fluid contains a large number of Cl^-, HCO_3^-, and other corrosion ions, which makes the working environment of the sucker rod worse and the corrosion fatigue failure increasingly serious [6–9]. The failure-free working time of the pumping rod is reduced, which cannot meet the requirements of continuous and stable production and depressurization of coal bed methane wells, and seriously affects the economic benefits of coal bed methane wells. Therefore, it is of great significance to study the corrosion fatigue characteristics of the sucker rod under the coupling effect of alternating load and corrosion damage of well fluid to prevent and reduce the field accidents caused by corrosion fatigue damage of sucker rod and improve the operation efficiency of coal bed methane wells [10–13].

Research on corrosion fatigue includes corrosion fatigue life prediction and the influence of frequency, stress amplitude, stress ratio, corrosion medium, temperature, etc., on corrosion fatigue life [13–26]. Researchers have proposed the Paris model and the Form model for prediction of fatigue life of sucker rods and the method for estimating fatigue characteristics by measuring mechanical properties of sucker rod materials [27,28]. The corrosion fatigue test with a solid sucker rod is the most direct and effective method to study the corrosion fatigue characteristics of high-strength sucker rod in a corrosive well fluid environment, but this will require a large testing machine and a long test cycle. At present, there are no conditions to test in the laboratory with the large sucker rod used in the oil well or coal bed methane sites [29]. The corrosion fatigue test of simulation sample pieces can better relieve the requirements of large test machine, but it still requires a long test cycle. Due to the restrictions of test conditions, the research on the corrosion fatigue performance of sucker rod is still limited, which cannot support the design of sucker rods. At present, the main test method to study the fatigue of sucker rod is the high-frequency fatigue test. For example, take a sine waveform with frequency as 10 Hz and a stress ratio at 0.1 to conduct high-frequency fatigue test at room temperature to obtain the corrosion fatigue characteristics of D-grade and H-grade sucker rods [30]. The frequency of hundreds of Hz or even thousands of Hz is generally adopted for the high frequency fatigue test, but the impulse of coalbed gas wells is $3–5 \text{ min}^{-1}$ in general, and the working frequency of sucker rod is about 0.05~0.084 Hz. The frequency adopted for the high frequency fatigue test is far more than the actual working condition of sucker rods [31]. In the deep coal bed methane well, the pump speed is low under actual working conditions, and the service state of the pumping rod is typical low-frequency and high-cycle corrosion fatigue. Previous studies have shown that as the frequency decreases, the exposure time of cracks in the air increases at each cycle, and the thickness of the oxide film generated by the sliding steps at the crack tip increases, thereby increasing the hindrance effect on the alternating shear process and increasing the fatigue crack propagation rate. This indirectly proves that frequency has an impact on fatigue life [32–34]. In addition, the frequency will affect the crack growth rate, and the corrosion at the crack tip will accelerate the crack initiation and growth on the surface of the sucker rod, indicating the correlation between the corrosion fatigue results and the frequency [35,36]. The current research has not fully considered the coupling effect of well fluid corrosion and alternating stress on the sucker rod during production, and there is a certain gap between the selection of corrosion medium and loading frequency and the actual working condition of sucker rods.

This research aims at the H-grade ultra-high-strength 4330 sucker rod commonly used in coal bed methane wells. Through the low-frequency and high-cycle corrosion fatigue test under different typical corrosion media, temperature, and stress levels, the corrosion fatigue life of 4330 sucker rod under different influence factors is obtained. This is expected

to provide the basis for the design of high strength sucker rod strings in deep coal bed methane wells under high-salinity well fluid working conditions.

2. Materials and Methods

2.1. Experimental Equipment and Materials

The main experimental equipment of the corrosion fatigue test is a WDML-10 slow-rate tensile testing machine from the Lichuang company in Xi'an, China; the waveform of the test is sine wave. The process and working principle of the corrosion fatigue test are shown in Figure 1.
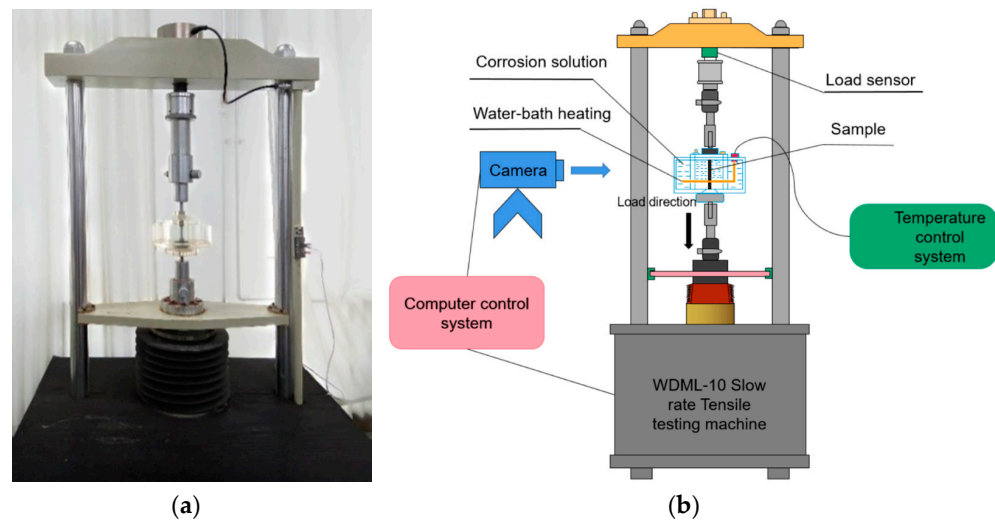

| (**a**) | (**b**) |

Figure 1. WDML-10 Slow rate tensile testing machine: (**a**) Photo of corrosion fatigue test process; (**b**) Operating principle diagram of corrosion fatigue testing machine.

The corrosion medium simulates the underground corrosion environment in the plexiglass vessel; the sample of the sucker rod passes through the corrosion vessel, the sample is immersed in the corrosion solution, and the part contacting with the vessel is sealed to prevent leakage of the corrosion solution. The corrosion circulation system consists of three parts: the corrosion medium storage, corrosion medium heater, and temperature control system. The structure principle is shown in Figure 2.
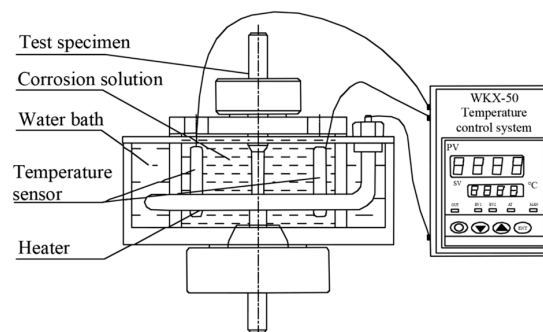

Figure 2. Corrosion fatigue test cycle system.

In order to be closer to the actual sucker rod, the test samples are all bar samples, and the axial loading stress is used to ensure that the simulated stress is closer to the actual stress. The sample material used in the test is the 4330 steel material widely used in coalbed gas wells at present. The sample is directly cut from 4330 sucker rod. Its material composition and heat treatment process are the same as the actual sucker rod used on site. The size of the sample was determined according to the provisions of the stress corrosion

sample in the NACE TM 0177-2016 standard [37] of the National Association of Corrosion Engineers. The detailed dimensions are shown in Figure 3.
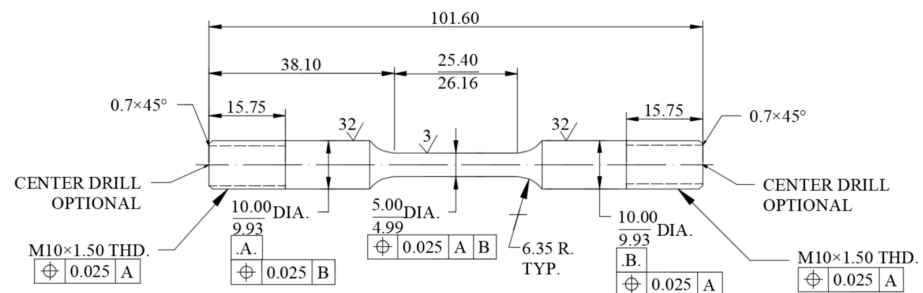

Figure 3. Detailed dimensions of the 4330 sucker rod test samples.

According to the standard ISO 6892-1:2019 [38], uses a tensile testing machine to break the un-corroded sucker rod sample and calculate the tensile strength σ_b. The photo before and after the 4330 control sample of sucker rod is broken is shown in Figure 4. The sample has obvious necking, smooth fractures, and typical cup-cone shape.
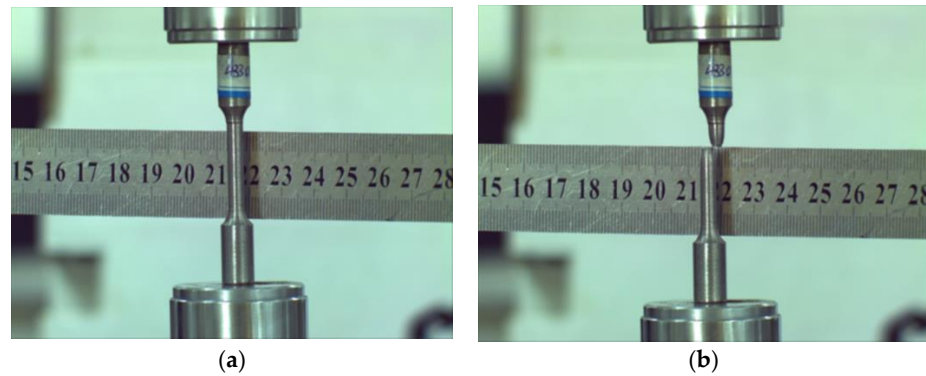

Figure 4. The tensile test of no corrosive 4330 sucker rod samples: (**a**) Before breaking; (**b**) After breaking.

The tensile force-displacement curves of the 4330 sucker rod specimens before the corrosion experiments as a control are shown in Figure 5.
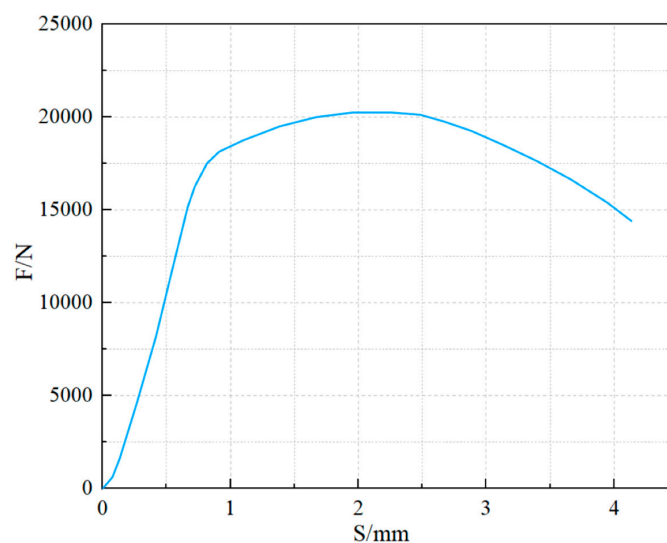

Figure 5. Tensile force-displacement curve of the 4330 sucker rod samples with no corrosion.

The parameters and main chemical compositions of 4330 sucker rod specimens are shown in Tables 1 and 2.

Table 1. The tensile strength of 4330 sucker rod samples.

Sample Material	Diameter /mm	Tensile Strength (σ_b)/MPa	Elongation Rate (δ)/%	Reduction of Area (Ψ)/%	Density (ρ)/m³·kg⁻¹	Elastic Modulus €/GPa
4330	4.961	1080	>10	>45	7850	209

Table 2. Chemical composition of 4330 sucker rods/%.

Material	C	Mn	P	S	Si	Cr	Mo	Ni	V
4330	0.3~0.36	0.40~0.60	≤0.015	≤0.010	0.15~0.35	0.90~1.20	0.4~0.50	2.75~3.00	0.05~0.1

From the tensile test results in Table 1, it can be seen that the tensile strength of 4330 sucker rod material is up to 1080 MPa, the elongation of the sample after breaking is more than 10%, and the section shrinkage is more than 45%, with good strength and plasticity.

The water content of the oil well in this block is more than 90%, the mineralization of the produced liquid is high, and the concentrations of Cl^-, HCO_3^-, and Ca^{2+} are greatly increased. The annual scrap rate of the sucker rod is more than 10%, and the maintenance work of the sucker rod accounts for nearly 1/3 of the total maintenance workload.

Through investigations on 4330 sucker rod used in coalbed gas well sites in a block, it is found that although 4330 sucker rod has a high tensile strength, its corrosion fatigue life in high-salinity well fluid is not in direct proportion to its static strength, and its service life in some wells is even lower than that of general sucker rod, only about 150 days on average, far from reaching the design standard. In the deep coal bed methane well A with high mineralization in the sampling block, the 4330 sucker rod fractured after 97 days of use, and the appearance of the broken rod is shown in Figure 6.

Figure 6. Fracture morphology of broken 4330 sucker rod in A well.

2.2. Design for Corrosive Media Selection

The corrosion medium for the corrosion fatigue test is determined based on the water quality analysis of the test block, the significance analysis of the impact of corrosion ions on the sucker rod, and the analysis of ion corrosion mechanism.

To bring the experimental conditions more in line with the real working conditions of the pumping rod site and to better design the corrosive solution medium, the well fluids of 400 wells in a block were extracted and analyzed for the medium ions contained in the well fluids. The analysis results are as follows: the main medium ions contained in the well fluids of the 400 wells in the field are Cl^-, HCO_3^-, Ca^{2+}, Mg^{2+}, Na^+, and K^+. The most

prevalent and high content of ionic media in the highly mineralized well fluids at the site is Cl^-, whose concentration distribution interval is mainly in the range of 0~20,000 mg/L, and HCO_3^- concentration distribution interval is mainly in the range of 0~800 mg/L. The concentration distribution of Cl^- and HCO_3^- ions in the data of 400 well fluids is shown in Figures 7 and 8.
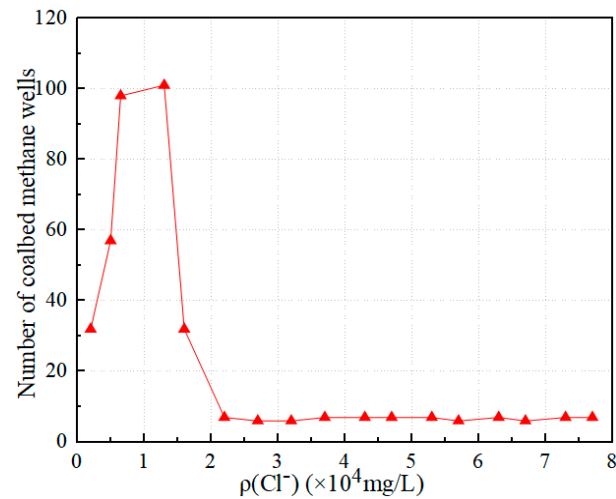

Figure 7. Concentration distribution of chloride ions in sampled well fluids.
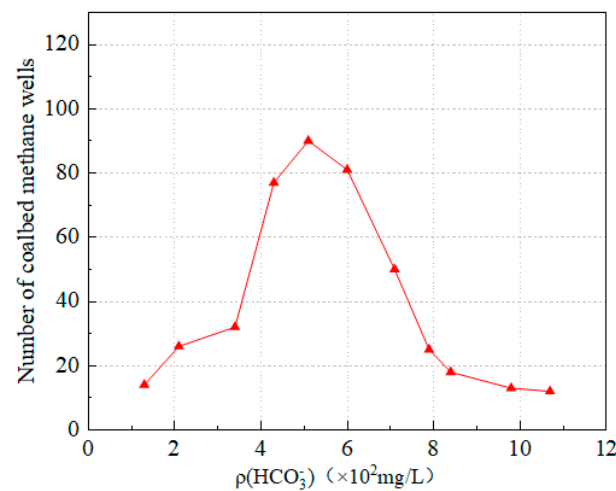

Figure 8. Concentration distribution of bicarbonate ions in sampled well fluids.

In the early years, our research group carried out the three-factor and three-level stress corrosion orthogonal test (L9 (3^4)) to study the stress corrosion sensitivity of 4330 sucker rod materials under the three corrosion media (Cl^-, HCO_3^-, and Ca^{2+}) [39]. Use elongation loss as the stress corrosion sensitivity evaluation index of test sample. The elongation loss is calculated according to the following equations:

$$I_\delta = \frac{\delta_a - \delta_c}{\delta_a} \times 100\% \tag{1}$$

where δ_a is the elongation of the material in the air and δ_c is the elongation of the material in the corrosive medium.

The experimental results were analyzed using the principle of orthogonal experiment; the experimental protocol and results are shown in Table 3.

Table 3. Stress corrosion orthogonal scheme and results for 4330 sucker rods.

No.	Factor				Test Result
	$\rho(Cl^-)$ /mg/L	$\rho(HCO_3^-)$ /mg/L	$\rho(Ca^{2+})$ /mg/L		
	Level				
	1	2	3	4	Elongation Loss I_δ
1	1 (10,000)	1 (0)	1 (200)	1	7.62%
2	1 (10,000)	2 (250)	2 (400)	2	15.51%
3	1 (10,000)	3 (500)	3 (600)	3	13.78%
4	2 (20,000)	1 (0)	2 (400)	3	20.14%
5	2 (20,000)	2 (250)	3 (600)	1	19.22%
6	2 (20,000)	3 (500)	1 (200)	2	14.81%
7	3 (30,000)	1 (0)	3 (600)	2	29.82%
8	3 (30,000)	2 (250)	1 (200)	3	21.37%
9	3 (30,000)	3 (500)	2 (400)	1	16.32%
I	36.91%	57.58%	43.8%		
II	54.17%	56.1%	51.97%		
III	67.51%	44.91%	62.82%		
K_1	12.303%	19.193%	14.6%		
K_2	18.057%	18.7%	17.323%		
K_3	22.503%	14.97%	20.94%		
R	10.2%	4.223%	6.34%		

In the orthogonal table, I, II, and III, respectively, represent the sum of elongation loss corresponding to the three levels; K_1, K_2, and K_3, respectively, represent the average elongation loss corresponding to the three levels; R represents the range, i.e., the difference between the maximum average elongation loss and the minimum average elongation loss. It can be seen from $K_3 > K_2 > K_1$ in the influence column of $\rho(Cl^-)$ and $\rho(Ca^{2+})$ that the higher the concentration of Cl^- and Ca^{2+}, the greater the elongation loss of 4330 sucker rod, and the positive relationship between the concentration of Cl^- and Ca^{2+} and the stress corrosion sensitivity of 4330 sucker rod. In the influence column of $\rho(HCO_3^-)$, $K_1 > K_2 > K_3$, indicating that the elongation loss of 4330 sucker rod decreases with the increase of HCO_3^- concentration. When HCO_3^-, Ca^{2+}, and Cl^- coexist, a certain concentration of HCO_3^- has a certain inhibition effect on the stress corrosion of Cl^- and Ca^{2+} of 4330 sucker rod. It can be seen from the range of R that the value of R corresponding to Cl^- concentration is the largest, which indicates that the elongation loss of 4330 sucker rod is most affected by the change of Cl^-, i.e., the stress corrosion sensitivity of 4330 sucker rod to Cl^- is the most significant.

Finally, the corrosion mechanism of each ion is analyzed. Ca^{2+} and Mg^{2+} have similar corrosion mechanisms to the sucker rod. They react with CO_2 in the well fluid or HCO_3^- with high concentration to generate $CaCO_3$, $MgCO_3$, and other carbonates. Scale and corrosion are generated on the surface of the steel rod column to form a thin film, resulting in passivation of the sucker rod surface. Due to uneven scaling and scaling and peeling off with reciprocating motion, local corrosion and pitting corrosion on the sucker rod surface are more severe. However, these two ions are not considered in this test due to their long influence period. Na^+ and K^+ have very high activity and almost do not participate in the corrosion behavior of the rod string in the well fluid, so their influence is not considered in the experiment in this paper.

Based on the above water quality analysis, the significance analysis of the impact of corrosion ions on the sucker rod and the analysis of the corrosion mechanism of ions, it is preferable that the corrosion media for corrosion fatigue test of 4330 sucker rod are Cl^- and HCO_3^-.

In the early stage, the research group carried out elongation loss and absorption work loss tests of different materials, as shown in Table 4.

Table 4. Elongation and absorbed work loss statistics of two materials after stress corrosion.

Test Number	ρ(Cl$^-$)/mg/L	ρ(HCO$_3{}^-$)/mg/L	4330		30CrMoA	
			Elongation Loss/%	Absorbed Work Loss/%	Elongation Loss/%	Absorbed Work Loss/%
1	5000	0	13.88	19.40	7.49	8.21
2	10,000	0	14.08	20.36	9.09	11.31
3	15,000	0	25.65	32.02	7.99	10.95
4	20,000	0	41.51	47.98	13.38	16.79
5	25,000	0	45.90	53.21	15.47	17.50
6	40,000	0	49.25	56.24	17.64	18.96
7	15,000	200	47.54	34.95	18.00	12.32
8	15,000	400	35.60	24.00	15.42	10.84
9	15,000	600	2.25	1.37	12.34	10.00
10	15,000	800	1.98	1.23	11.99	9.23

2.3. Design of Corrosion Fatigue Test Conditions

For the service condition of 4330 pumping rods, due to its obvious low-frequency and high-frequency corrosion fatigue characteristics, as well as to shorten the corrosion fatigue test period as much as possible, and to improve the reliability of the measurement results as much as possible, the maximum stress σ_{max} of the corrosion fatigue test is set to 70% σ_b by adopting the standard of NACE TM 0177-2016 [29]. At the same time, taking into consideration the actual use situation, the stress ratio is set to 0.6 to improve the reliability and maneuverability of the measurement results. In the fatigue experiment, the minimum stress σ_{min} is set to 42% σ_b; in order to simulate the actual working condition of the pumping rods in deep coalbed methane wells, the experimental frequency is taken as 0.05 Hz.

3. Results and Discussion

Low-frequency high-frequency corrosion fatigue experiments were carried out under different Cl$^-$ and HCO$_3{}^-$ concentrations, with the main purpose of elucidating the corrosion fatigue life characteristics of 4330 sucker rods in different corrosive solutions. At the same time, the corrosion fatigue law of 4330 pumping rods under different temperature and stress level conditions was investigated, and the experimental results are as follows.

3.1. 4330 Corrosion Fatigue Experiments on Pumping Rods in Different Corrosive Solutions
3.1.1. 4330 Corrosion Fatigue Experiments on Pumping Rods at Different Cl$^-$ Concentrations

As can be seen from Table 4, the loss of elongation and work of absorption increased with the increase of ρ(Cl$^-$), but the loss of elongation were both lower and the loss of work of absorption were smaller when ρ(Cl$^-$) was lower than 10,000 mg/L, the loss of elongation and work of absorption increased sharply when ρ(Cl$^-$) reached 15,000 mg/L, and continued to increase when ρ(Cl$^-$) reached 25,000 mg/L, but leveled out. In order to verify the trend, ρ(Cl$^-$) = 40,000 mg/L was chosen as a supplement. From the original Figure 7, it can be seen that the gas wells with ρ(Cl$^-$) below 25,000 mg/L comprise more than 95% of the total number of gas wells, and the effect of Cl$^-$ on the stress corrosion susceptibility of the material does not change much when it reaches more than 25,000 mg/L, so 0–25,000 mg/L is selected as the range of Cl$^-$.

Seven sets of experiments were designed in the range of Cl$^-$ concentration of 0–40,000 mg/L. The group with a Cl$^-$ concentration of 0, i.e., the specimen experimented in air, was used as the control group, and the results obtained were set as the fatigue life of 4330 pumping rods in a corrosion-free environment. According to the principle of probability, each experiment was repeated three times to take the average value. The experimental results are shown in Table 5.

Table 5. Corrosion fatigue test results of 4330 sucker rod under different $\rho(Cl^-)$.

$\rho(Cl^-)$/mg/L	σ_{max}/Mpa	σ_{min}/Mpa	Stress Ratio	$N \times 10^4$			$\overline{N} \times 10^4$	σ^2
0	750	450	0.6	24.30	22.42	22.09	22.94	0.947
1000	750	450	0.6	9.81	8.56	7.93	8.77	0.610
3000	750	450	0.6	9.50	8.54	8.03	8.69	0.371
5000	750	450	0.6	7.52	6.98	4.11	6.20	2.240
10,000	750	450	0.6	7.22	6.70	5.81	6.58	0.339
25,000	750	450	0.6	8.35	7.83	6.48	7.55	0.621
40,000	750	450	0.6	6.82	6.11	5.81	6.25	0.179

$\overline{N}$ is the average fatigue life, σ^2 is the variance.

According to the corrosion fatigue life N and the average life $\overline{N}$ under different $\rho(Cl^-)$, the variance values of each group were calculated, respectively, and it was found that only one group of data had a variance of more than 1; the other groups had a variance of less than 1, which ensured the reliability of the data in repeated experiments.

According to the average life results of corrosion fatigue experiments of 4330 pumping rod specimens under different Cl^- concentrations, as shown in Table 5, the corrosion fatigue life curves of 4330 pumping rod specimens were fitted and shown in Figure 9.
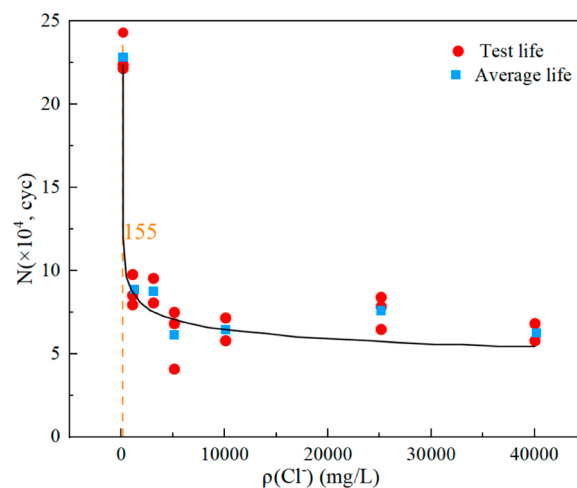
Figure 9. Corrosion fatigue life of 4330 sucker rod specimens at different $\rho(Cl^-)$.

Analysis of Table 5 shows that when the maximum stress is 750 MPa, the fatigue life of the 4330 sucker rod is in the range of 200~250,000 times under the environment of no corrosion, but when Cl^- exists in the solution, the fatigue life of 4330 sucker rod specimens decreases dramatically, which are in the range of 60~90,000 times, and the fatigue life under the environment of no corrosion is nearly an order of magnitude different. From Figure 9, it can be seen that with the increase of Cl^- concentration, the corrosion fatigue life of 4330 sucker rod gradually decreases, but the trend gradually slows down. This law of Cl^- is consistent with a large number of existing research results [28]. Usually, metal materials undergo oxidation reactions in corrosive environments, and the oxidation product film protects the metal surface from further corrosion damage. The effect of cyclic stress will cause the oxide film on the material surface to rupture, exposing the metal surface to the corrosive medium again, and the corrosion continues and gradually evolves into corrosion pits. Numerous studies [40,41] have shown that the form of corrosion damage caused by Cl^- on metal materials is pitting corrosion. Usually, the Cl^- radius is small, so it can easily pass through the gap of the passivation film and enter the inner layer, reacting with exposed fresh metal to form soluble compounds, thereby inducing pitting damage. In the case where the crack tip is covered by a passivation film, the film here is more prone to rupture due to stress concentration. When the concentration of Cl^- increases from 0 to

155 mg/L, the adsorption effect of Cl^- on the product film is also enhanced, and Cl^- will adsorb at the weak point of the oxidation film layer and cause local damage to the oxidation film, further reacting with the fresh metal surface and exacerbating corrosion damage, significantly reducing the corrosion fatigue life of the material. When the concentration of Cl^- reaches 10,000 mg/L, the Cl^- in the solution approaches saturation, and the product film on the metal surface thickens, hindering the penetration of Cl^- and slowing down the corrosion process. When the Cl^- concentration reaches the threshold value of 155 mg/L, the corrosion fatigue life of 4330 sucker rods sharply decreases. When the threshold value of 155 mg/L is exceeded, the change of Cl^- concentration in the corrosion solution has little effect on the corrosion fatigue life of 4330 sucker rod, and the service life was stable at about 6.2×10^4 times.

This also indicates that the size of Cl^- concentration is not a significant factor affecting the corrosion fatigue life of 4330 sucker rod material, but, as long as Cl^- exists, even if it exists at a low concentration (exceeding the threshold value of 155 mg/L), it will significantly reduce the fatigue life of 4330 sucker rod. This provides a basis for the fatigue load design of sucker rods in Cl^- containing well fluids.

3.1.2. 4330 Corrosion Fatigue Experiments on Sucker Rods at Different HCO_3^- Concentrations

As can be seen from Table 4, HCO_3^- has a greater influence on the elongation loss and work of absorption loss of sucker rods within the range of 0–600 mg/L. When $\rho(HCO_3^-)$ is greater than 600 mg/L, the change of plasticity loss of the material tends to be stabilized, and elongation loss and work of absorption loss of the material tends to be zero, and plasticity and work of absorption loss of the material are suppressed to a large extent, and it is not significant to continue to increase $\rho(HCO_3^-)$. Meanwhile, according to the distribution of HCO_3^- in the field well fluids, the $\rho(HCO_3^-)$ in most wells is below 600 mg/L, so 0–600 mg/L is selected as the range of HCO_3^-.

Many studies have shown that HCO_3^- has passivation effect, which makes the passivation film thicken and the anode current density decreas, so the metal stays blunt. However, Cl^- has an erosion effect, which will thin the passive film or increase the ion conductivity, increase the anode current density, lose the metal passivity, and aggravate the corrosion [42–44]. When $\rho(HCO_3^-)$ is in the range of 0–600 mg/L, HCO_3^- inhibits the stress corrosion of Cl^-, and when $\rho(HCO_3^-)$ exceeds 600 mg/L, the inhibition of HCO_3^- on the stress corrosion of Cl^- is weakened, and thus the coexistence of HCO_3^- and Cl^- in alkaline environments does not improve the fatigue life of the material.

Meanwhile, the effect of HCO_3^- on the stress corrosion of the material is related to the type of material. When $\rho(HCO_3^-)$ is in the range of 0–600 mg/L, increasing $\rho(HCO_3^-)$ can inhibit the stress corrosion of 4330 in $C1^-$ containing solution. However, the inhibition effect on 30CrMoA was not obvious, and 30CrMoA performed more stable and better than 4330 in the same test environment. In addition, more than 90% of the well fluids sampled in this study all contain Cl^- and HCO_3^- at the same time. Therefore, in order to ensure that the test conditions are consistent with the field well fluids, the test is designed for the effect of the combined action of HCO_3^- and Cl^- on the corrosion fatigue life of the sucker rod materials. A corrosive medium solution is designed as the mixed solution, with a different concentration of HCO_3^- and constant concentration of 15,000 mg/L Cl^-. The 4330 sucker rod sample is put into the solution of mixed corrosive medium for the corrosion fatigue test, and the corrosion fatigue life test results are shown in Figure 10.

According to the results of Figure 10, the corrosion fatigue life of the 4330 sucker rod material is the highest, which can reach 75,000 times when the concentration of HCO_3^- in the mixed solution is 0 with the same concentration of Cl^-. However, the corrosion fatigue life of 4330 sucker rod material decreases gradually with the increase of HCO_3^- concentration. When $\rho(HCO_3^-)$ continues to increase by more than 600 mg/L, the corrosion fatigue life of 4330 sucker rod is stable at around 6×10^4 times. From the experimental results, it can be seen that the corrosion fatigue life of the 4330 sucker rod further decreased

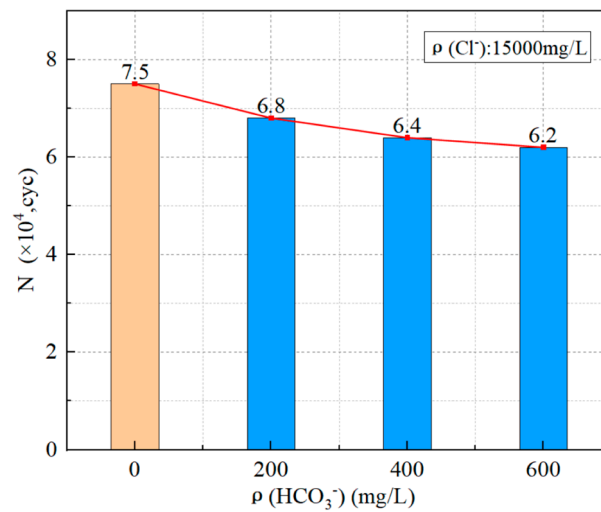when HCO_3^- and Cl^- coexisted, and the presence of HCO_3^- had an unfavorable effect on its corrosion fatigue life.

Figure 10. Corrosion fatigue life of 4330 sucker rod specimens in different $\rho(HCO_3^-)$.

3.2. 4330 Corrosion Fatigue Experiments on Pumping Rods at Different Temperature Conditions

Temperature plays an important role in influencing the corrosion fatigue life of sucker rod materials. In deep coalbed methane wells, the temperature at the bottom of the well differs greatly from the wellhead temperature due to the influence of the ground temperature gradient. According to the data of the research sampling block, the down-pumping depth of the CBM wells in this block is mostly concentrated in the range of 1500–2500 m, and the ground temperature gradient is in the range of 2.8–3.2 °C/hm, which can be obtained that the working temperature range of the bottom pumping rods in this block is about 70–90 °C. To study the influence law of temperature on the corrosion and fatigue life of 4330 pumping rod material, four different temperature levels were selected to design the experiment, which was room temperature (25 °C), 50 °C, 70 °C, and 90 °C. According to the principle of consistency of experimental conditions, a mixed solution of 25,000 mg/L Cl^-, 600 mg/L HCO_3^-, and a medium consistent with the field well fluid was used for the experiments; the experimental results are shown in Figure 11.
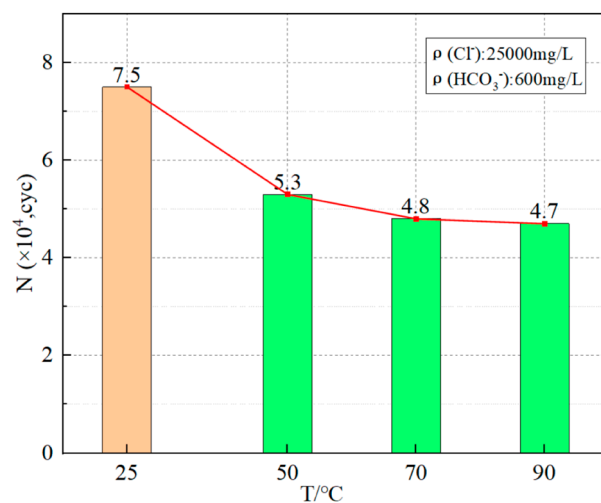

Figure 11. Corrosion fatigue life of 4330 sucker rod samples at different temperatures.

According to the law of Figure 11, the temperature has a significant effect on the corrosion fatigue life of 4330 sucker rod material; with the gradual increase of the tem-

perature in the corrosive environment, its corrosion fatigue life gradually decreases, and the decreasing trend is first significant and then gradually slows down. The corrosion fatigue life of 4330 sucker rod in the solution containing 25,000 mg/L Cl^- and 600 mg/L HCO_3^- was 75,000 times when the temperature was 25 °C, but the corrosion fatigue life was 53,000 times, 48,000 times, and 47,000 times when the temperature was 50 °C, 70 °C and 90 °C, respectively. The increase of $\rho(Cl^-)$ leads to the formation of a passivation film on the surface of the material or accelerates the destruction of the passivation film, thereby promoting local corrosion. With the increase of temperature, the activity of Cl^- increases, and its effect on the fatigue life of the material intensifies. As a result, the temperature promotes the corrosive effect of Cl^- on the 4330 sucker rod material, further reducing its corrosion fatigue life. As can be seen from Figure 11, the effect of temperature on accelerating the corrosive effect of Cl^- is more significant in the temperature range of 25–70 °C. When the temperature continues to rise, that is, when the temperature is greater than 70 °C, the significance of its influence gradually reduces, and 4330 sucker rod corrosion fatigue life tends to stabilize.

Research has shown [45,46] that an increase in temperature is beneficial for the electrochemical reaction of corrosion, as the resistance of the electrolyte solution decreases with the increase in temperature, accelerating the cathodic and anodic processes. Therefore, when the temperature rises to 50 °C, corrosion intensifies, leading to a decrease in corrosion fatigue life. On the other hand, as the temperature increases, the oxygen content in the solution decreases (the solubility decreases after the temperature increases). When the temperature exceeds 70 °C, in the case of oxygen depolarization corrosion, it is not conducive to corrosion and the corrosion fatigue life gradually stabilizes around 4.7×10^4 times.

3.3. 4330 Corrosion Fatigue Experiments on Pumping Rods at Different Stress Levels

During the corrosion fatigue process, the sucker rod is subjected to alternating stresses, and the formation of etch holes, etch pits, or corrosion notches can also lead to stress concentration. The generation of more and more cracks on the surface of the sucker rod is also due to the corrosion at the crack tip and a variety of etch holes will also be randomly formed on its surface, which also makes the fracture show multiple crack sources [47], as shown in Figure 12.

Figure 12. Corrosion fatigue fracture surface of 4330 sample.

To study the corrosion fatigue law of 4330 sucker rod material under different stress levels, low-frequency corrosion fatigue experiments were carried out at different stress levels, i.e., different working maximum loads, and the concentration of Cl^- in the exper-

imental solution was selected as 10,000 mg/L, and the experimental design scheme and results are shown in Table 6. According to the experimental results in the table, it can be seen that the corrosion fatigue life of the 4330 pumping rod increases gradually with the reduction of the maximum load under the constant ion content and temperature of the solution. When stress levels are reduced to 530 MPa, corrosion fatigue life can be up to 228,800 times.

Table 6. Corrosion fatigue test results of 4330 sucker rod under different stress levels.

Material	$\rho(Cl^-)$/mg/L	S/MPa	Stress Ratio	$N \times 10^4$
4330	10,000	530	0.6	22.88
4330	10,000	600	0.6	14.96
4330	10,000	640	0.6	15.31
4330	10,000	700	0.6	9.92
4330	10,000	750	0.6	6.58

At a stress level of 750 MPa, the corrosion fatigue life is up to 65,800 times. At this time, the stress level continues to increase, and the corrosion fatigue life does not change much. The corrosion fatigue life of 4330 sucker rod material can be prolonged by the measure of reducing the stress level suffered by the sucker rod when working, but this measure is not applicable in the wells requiring strong pumping with large pumps and deep pumping with small pumps.

The data in Table 6 were fitted (limited data results due to experimental conditions and time constraints) as shown in Figure 13. The equation for the S-N curve of 4330 sucker rod under low-frequency corrosion fatigue in a corrosive well fluid environment was obtained as:

$$\lg N = 11.64 - 3.77 \lg S \tag{2}$$

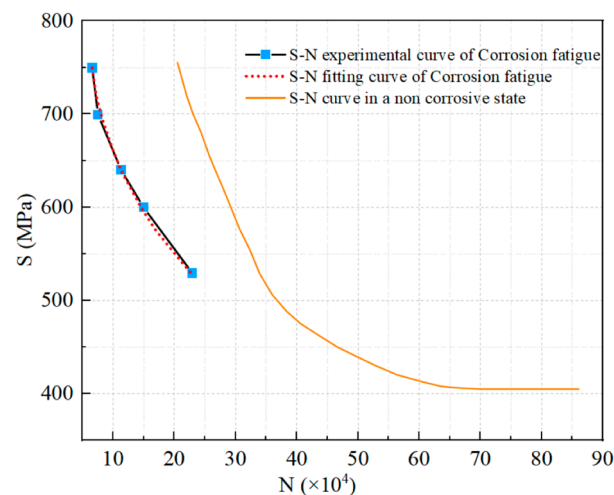where N is the fatigue life $\times 10^4$ and S is the stress, MPa.

Figure 13. Corrosion fatigue life of 4330 sucker rod under different stress levels.

At present, the infinite life fatigue design method is used to calculate the strength of the sucker rod, that is, when the service life of the sucker rod reaches 10^7, the default rod body reaches infinite life. According to the fitting Formula (2), when N is 10^3, S is 195.78 MPa, so the fatigue limit of 4330 sucker rod under the corrosion environment and stress ratio of 0.6 at room temperature (25 °C) in 10,000 mg/L Cl$^-$ solution is 196 MPa. It can also be seen from Figure 13 that the corrosion fatigue life curve significantly reduces the stress level at the same fatigue life compared to the non-corrosion fatigue life curve, which is expected to provide the basis for the stress load design of the sucker rod in the corrosion environment.

The above studies show that temperature is the main factor affecting the fatigue life of locally corroded steel, followed by stress level, and the fatigue life of steel decreases with the increase of stress level. Proper heat treatment can be used to improve the alloy structure, reduce the gas content, eliminate residual stresses, and improve the corrosion resistance of the material.

4. Conclusions

1. The corrosion fatigue life of 4330 sucker rod gradually decreases with the increase of Cl^- concentration. When the Cl^- concentration is higher than the threshold value of 155 mg/L, the corrosion fatigue life of 4330 sucker rod sharply decreases. When this threshold is exceeded, the downward trend slows down. The significant factor affecting the corrosion fatigue life of 4330 material is not the concentration of Cl^- but the existence of Cl^-. The corrosion fatigue life of 4330 sucker rod is further reduced when HCO_3^- and Cl^- coexist, and the existence of HCO_3^- has an adverse impact on its corrosion fatigue life.

2. The temperature promotes the effect of Cl^- on the corrosion fatigue life of 4330 sucker rod. With the increase of temperature, the corrosion fatigue life of 4330 sucker rod decreases gradually. When the well fluid temperature is lower than 50 °C, the effect of temperature on the corrosion fatigue life of sucker rod is more significant; When the temperature of well fluid exceeds 70 °C, the decline trend of corrosion fatigue life slows down.

3. Through the corrosion fatigue test of 4330 sucker rod under different stress levels, the low-frequency corrosion fatigue S-N curve under corrosion environment is obtained. Based on the fitted S-N curve (stress-fatigue life curve), the fatigue limit of 4330 sucker rod in 10,000 mg/L Cl^- solution at room temperature is calculated as 196 MPa at stress ratio of 0.6. Under the same fatigue life, the stress level under the corrosive environment is greatly reduced compared with the non-corrosive environment. It provides a basis for the stress load design and corrosion fatigue life prediction of sucker rod under high salinity conditions.

References

1. Hu, A.M.; Qi, Y.G. *Theoretical Exploration and Engineering Practice of Coal Bed Methane Development*, 1st ed.; China University of Petroleum Press: Qingdao, China, 2014; pp. 1–19.
2. Jia, B.; Xian, C.-G. Permeability measurement of the fracture-matrix system with 3D embedded discrete fracture model. *Pet. Sci.* **2022**, *19*, 1757–1765. [CrossRef]

3. Vishnyakov, D.; Solodkiy, E.; Alnico, S. Improving Sucker-rod pump energy efficiency through electric drive movement control. In Proceedings of the 2021 28th International Workshop on Electric Drives: Improving Reliability of Electric Drives (IWED), Moscow, Russia, 27–29 January 2021; pp. 1–3.

4. Li, D.J.; Wang, W.; Pang, B.; Lin, W.; Li, W.Z.; Ji, L.; Feng, Y.R. Influence factors on corrosion fatigue life of sucker rods used in coalbed methane well. *Trans. Mater. Heat Treat.* **2017**, *38*, 121–127.

5. Tskacs, G. *Sucker-Rod Pumping Handbook: Production Engineering Fundamentals and Long-Stroke Rod Pumping*; Gulf Professional Publishing: Amsterdam, The Netherlands, 2015; pp. 15–19.

6. Wang, Y.H. Application of HY grade ultra-high strength sucker rod in Wennan Oilfield. *Energy Conserv. Pet. Petrochem. Ind.* **2019**, *9*, 63–65.

7. Lei, T.Q. A review of corrosion fatigue studies on high strength steels. *J. Shandong Electr. Power High. Spec. Sch.* **2021**, *24*, 48–52+62.

8. Wang, Z.L. A Design Method for Extending Fatigue Life of Pumping Rod Based on Stress Ratio. *Unconv. Oil Gas* **2023**, *10*, 127–134+142.

9. Alireza, B.; Meysam, H. A critical review on very high cycle corrosion fatigue: Mechanisms, methods, materials, and models. *J. Space Saf. Eng.* **2023**, *10*, 284–323.

10. Fujii, T.; Sawada, T.; Shimamura, Y. Nucleation of stress corrosion cracking in aluminum alloy 6061 in sodium chloride solution: Mechanical and microstructural aspects. *J. Alloys Compd.* **2023**, *938*, 168583. [CrossRef]

11. Chen, G.X.; Wang, M.J.; Cui, C.X. Corrosion-Fatigue Life Prediction of the U-Shaped Beam in Urban Rail Transit under a Chloride Attack Environment. *Materials* **2022**, *15*, 5902. [CrossRef]

12. Morgantini, M.; MacKenzie, D.; Comlekci, T. The Effect of Mean Stress on Corrosion Fatigue Life. *Procedia Eng.* **2018**, *213*, 581–588. [CrossRef]

13. Zhu, Y.M.; Chen, J.J.; Tang, W.X. Fatigue and Corrosion Fatigue of 18Ni Maraging Steel. *Arch. Metall. Mater.* **2021**, *66*, 381–390.

14. Al-shawish, T.A.M. Study on the Corrosion Resistance and Fatigue Performance of High Chromium Alloy Steel Sucker Rods. Master's Thesis, China University of Petroleum (East China), Shanghai, China, 2021.

15. Tian, G.; Yi, Y.G.; Han, X.; Cai, L.L.; Yu, H.Y.; Zeng, D.Z. Corrosion Law and Corrosion Prediction of Sucker Rod in CO_2 Composite Steam Flooding Production Well. *Corros. Prot.* **2021**, *42*, 21–26.

16. Santos, E.A.; Giorgetti, V.; Souza Junior, C.A.; Marcomini, J.B.; Sordi, V.L.; Rovere, C.A. Stress corrosion cracking and corrosion fatigue analysis of API X70 steel exposed to a circulating ethanol environment. *Int. J. Press. Vessel. Pip.* **2022**, *200*, 104846. [CrossRef]

17. Di Egidio, G.; Tonelli, L.; Morri, A.; Boromei, I.; Shashkov, P.; Martini, C. Influence of Anodizing by Electro-Chemical Oxidation on Fatigue and Wear Resistance of the EV31A-T6 Cast Magnesium Alloy. *Coatings* **2023**, *13*, 62. [CrossRef]

18. Su, W.; Zhu, H.M. In situ corrosion fatigue life of 2198-T8 Al–Li alloy based on tests and DIC technique. *Mater. Test.* **2022**, *64*, 1383–1396. [CrossRef]

19. Huang, L.; Zheng, S.; Qin, Y.; Han, J.; Qiao, Y.; Chen, J. Corrosion Behavior of Selective Laser Melted Ti-6Al-4V in 0.1 mol/L NaOH Solution. *Coatings* **2023**, *13*, 150. [CrossRef]

20. Schönowitz, M.; Maier, B.; Grün, F.; BauerTroßmann, K. Influence of corrosion fatigue on the fatigue strength of an AlSi10MgMn high-pressure die-casting alloy with regard to the surface condition. *Mater. Corros.* **2023**, *74*, 1382–1389. [CrossRef]

21. Olumide, T.O.; Olamide, B.O.; Timothy, O.O.; Adeyeri, M.K. Stress-Corrosion and Corrosion-Fatigue Properties of Surface-Treated Aluminium Alloys for Structural Applications. *Chem. Afr.* **2023**, *6*, 1699–1708.

22. Chen, Z.Y.; Zhu, Z.L.; Wang, B.H.; Ma, C.H.; Liu, Y.T.; Khan, H.I.; Pan, P.; Zhang, T.; Wang, X.; Zhang, N. Effect of different loading conditions on corrosion fatigue crack growth rate of a nickel-based alloy in supercritical water. *Int. J. Fatigue* **2023**, *175*, 107815. [CrossRef]

23. Kret, N.V.; Svirska, L.M.; Venhrynyuk, T.P. Corrosion-Fatigue Crack Propagation in Exploited Pump Rods Made of 20N2M Steel. *Mater. Sci.* **2020**, *56*, 279–283. [CrossRef]

24. Marcus, W.; Anja, P. Corrosion Fatigue of Standard Duplex Stainless Steel X2CrNiMoN22-5-3 under Rotation Bending Load in Northern German Basin Environment. *Solid State Phenom.* **2023**, *6918*, 71–76.

25. Knysh Vitalii, V.; Mordyuk Bohdan, N.; Solovei Sergii, O.; Volosevich, P.Y.; Skoryk Mykola, A.; Lesyk Dmytro, A. Combining electric discharge surface alloying and high-frequency mechanic impact post-processing for increased corrosion fatigue life of as-welded transverse non-load-carrying attachments of the S355 steel. *Int. J. Fatigue* **2023**, *177*, 107926. [CrossRef]

26. Liu, M. Anatomy of the Goodman stress diagram method for determining the allowable stress of a pumping rod. *Oilfield Mach.* **1986**, *15*, 7–9.

27. Lin, Y.H.; Zhang, D.P.; Luo, F.Q. Study on fatigue life calculation of pumping rods. *Pet. Drill. Technol.* **2005**, *6*, 66–69+105.

28. Yang, C.H. Corrosion Fatigue Life Assessment and Reliability of Oil Well Pipes in Cl- Bearing Service Environment. Master's Thesis, Xi'an University of Petroleum, Xi'an, China, 2021.

29. Li, C. Stress Corrosion and Fatigue Properties of ZL101 Aluminum Alloy. Shanghai. Master's Thesis, Shanghai Jiao Tong University, Shanghai, China, 2011.

30. Yi, M. Development of 1000 MPa Grade Low Carbon Bainite Steel for Pumping Rod. Ph.D. Thesis, Northeastern University, Shenyang, China, 2015.

31. Ji, Z.G.; Yin, F.F. Testing the fatigue life of materials using a high-frequency fatigue tester. *Eng. Test.* **2008**, *3*, 7–9.

32. Liu, Z.; Li, Y.C.; Wang, Z.G.; Wang, Y.; Liu, C.Y. Effect of loading frequency and heat treatment on the fatigue crack expansion rate of die-cast magnesium alloy AZ91H. *J. Aerosp. Mater.* **2000**, *1*, 7–11.
33. Adedipe, O.; Brennan, F.; Kolios, A. Corrosion fatigue load frequency sensitivity analysis. *Mar. Struct.* **2015**, *42*, 115. [CrossRef]
34. Guo, C. Study on Fatigue Crack Expansion Rate and Life Prediction of 4130X Material Under Different Corrosion Conditions. Master's Thesis, Beijing University of Technology, Beijing, China, 2022.
35. Zhong, Y.; Shao, Y.B.; Gao, X.D.; Luo, X.F.; Zhu, H.M. Fatigue crack growth of EH36 steel in air and corrosive marine environments. *J. Constr. Steel Res.* **2023**, *210*, 108104. [CrossRef]
36. Chen, W.J.; Lu, W.; Gou, G.Q.; Dian, L.W.; Zhu, Z.Y.; Jin, J.J. The Effect of Fatigue Damage on the Corrosion Fatigue Crack Growth Mechanism in A7N01P-T4 Aluminum Alloy. *Metals* **2023**, *13*, 104. [CrossRef]
37. *NACE TM0177-2016*; Standard Test Method: Laboratory Testing of Metals for Resistance to Sulfide Stress Cracking and Stress Corrosion Cracking in H2S Environments. NACE International: Houston, TX, USA, 2005.
38. *ISO 6892-1:2019*; Metallic Materials—Tensile Testing—Part 1: Method of Test at Room Temperature. General Administration of Quality Supervision, Inspection and Quarantine of the People's Republic of China: Peking, China. Standardization Administration of the People's Republic of China: Peking, China, 2011.
39. Li, Y. The Research with Corrosion Resistance to Stress of Sucker Rod in High Water Conditions. Master's Thesis, China University of Petroleum (East China), Qingdao, China, 2014.
40. Polyanskiy, V.M.; Puchkov, Y.A.; Orlov, M.R.; Napriyenko, S.A.; Lavrov, A.V. lnfluence of tensile stresses on the corrosion resistance o f titanium alloy VT22 in aqueous solution of NaCI. *Inorg. Mater. Appl. Res.* **2017**, *8*, 94–99. [CrossRef]
41. Behera, P.K.; Katiyar, P.K.; Misra, S.; Mondal, K. Effect of Pre-induced Plastic Strains on the Corrosion Behavior of Reinforcing Bar in 3.5 pct NaCl Solution. *Metall. Mater. Trans. A* **2021**, *52*, 605–626. [CrossRef]
42. Liu, G.X.; Wu, M.; Xie, F. Effect of HCO_3^- on Electrochemical Corrosion Behavior of X100 Pipeline Steel in Marine Environment. *J. Petrochem. Univ.* **2019**, *31*, 66–70.
43. Zhou, T.Y.; Yu, Y.X.; Zhao, B. Study on the Pitting Corrosion of 20# Steel in HCO_3^- and Cl^- Mixed Solution. *Saf. Health Environ.* **2020**, *20*, 30–34.
44. Mangat, P.S.; Ojedokun, O.O. Bound chloride ingress in alkali activated concrete. *Constr. Build. Mater.* **2019**, *212*, 375–387. [CrossRef]
45. Zang, Q.S.; Liu, K.; Ma, M.Y. Effects of frequency, pH value, and temperature on the corrosion fatigue performance of A537 marine steel. *Corros. Sci. Prot. Technol.* **1989**, *2*, 10–14.
46. Gibson, G.J.; Perkins, K.M.; Gray, S.; Leggett, A.J. Influence of shot peening on high-temperature corrosion and corrosion-fatigue of nickel based superalloy 720Li. *Mater. High Temp.* **2016**, *33*, 225–233. [CrossRef]
47. Liang, Y.; Zhao, C.; Fan, S.; Lei, Y.; Shi, H.X. Experimental analysis of fatigue performance of sucker rods. *Equip. Environ. Eng.* **2019**, *16*, 39–42.